XPS analysis of carbon-supported platinum electrodes and characterization of CO oxidation on PEM fuel cell anodes by electrochemical half cell methods

J.M. Rheaume, B. Müller *, M. Schulze

Institute of Technical Thermodynamics, German Aerospace Research Center (DLR), Pfaffenwaldring 38-40, D-70569 Stuttgart, Germany

Abstract

An analysis using X-ray induced photoelectron spectroscopy (XPS) on an as received, 20 weight percent (wt.%) Pt/C electrode (E-TEK) indicates the presence of a nanometer thin layer of polytetrafluorethylene (PTFE) on the surface which degrades during potentiodynamic cycling from 0 to 1.5 V RHE. Half cell measurements verify this observation by exhibiting an increase in the transferred charge and thus active surface area. An electrode manufactured by a rolling process containing 20 wt.% Pt/C on a carbon cloth (catalysts powders and cloth from E-TEK) did not have such a layer according to XPS analysis or exhibit such behavior during electrochemical, potentiodynamic cycling. In addition, cyclic voltammetry in a half cell was used to characterize CO oxidation on these two electrodes in addition to one consisting of 20 wt.% Pt–Ru/C catalyst on a carbon backing also produced by the rolling process. Measurements in 0.5 M H_2SO_4 electrolyte of rotating disk electrodes (RDEs) show recognizable CO oxidation during stripping experiments at potentials comparable to those shown by smooth electrodes, although peak definition for supported electrodes is highly inferior. The labyrinth nature of the pore systems of supported electrodes complicated stripping measurements and called into question the benefit of using RDEs for porous electrodes due to undefinable mass transport conditions within the electrode. © 1998 Elsevier Science S.A. All rights reserved.

1. Introduction

The ability to meet the exploding demand for power is a formidable challenge facing the world on the brink of entering a new century. By the year 2010, 48% more energy will be required worldwide than in 1991 [1]. Renewable energy sources would be the ideal solution, but since the consumption of irreplaceable fossil fuels which meet the bulk of power needs nowadays is non-sustainable, worldwide attention focus on processes that convert these precious resources into electricity via efficient, economical and environmentally sound manners. Laboratories world-

wide race to develop highly promising technologies such as proton exchange membrane fuel cells (PEMFCs) which can produce electricity and heat via electrochemical reactions. Such devices can attain efficiencies above those of conventional combustion cycles which are limited by Carnot's efficiency.

PEMFCs that will obtain a high degree of public acceptance will likely consume reformed hydrocarbons or will directly transform methanol. In both of these cases, catalysts that oxidize CO are necessary to avoid the very large overpotentials necessary to oxidize the CO that preferentially adsorbs on Pt sites, blocking the access of H_2 to this catalyst. Therefore, an impetus exists to create CO tolerant electrodes. Some of the more promising candidates, including alloys of Pt with Ru and Sn, have already been well researched and documented [2–11].

The evaluation of carbon-supported catalysts in a fuel cell is a costly and time consuming process. Tamizhmani et al. recently reported that the relative activity of some CO-catalysts for oxygen reduction in half-cell measure-

ments in H_2SO_4 agreed with the those taken in a single cell [12]. Although the interactions between a catalyst supported on graphite and liquid H_2SO_4 of a half cell do not perfectly emulate those between a catalyst and a solid Nafion membrane of a full cell, this group found enough agreement on the relative activity to conclude that RDEs could be used to prescreen the more promising candidates for further study.

Our goal is to use similar half cell techniques to characterize CO oxidation on the graphite supported catalysts of our self-made porous electrodes in order to make comparisons with those of other manufacturers. In the following pages, we introduce our investigation of smooth Pt to verify the validity of our half cell assembly. In addition, we present our findings obtained via electro-oxidation experiments and XPS analysis about the degradation of a PTFE layer on the surface of on a commercially available 20 wt.% Pt/C electrode from E-TEK (Natick, MA, USA) which we compare with similar tests on an in-house made electrode with similar catalyst content. Furthermore, we discuss the results of CO stripping experiments performed on the E-TEK electrode and on self-manufactured, graphite-supported Pt and Pt–Ru electrodes in 0.5 M H_2SO_4 at room temperature.

2. Experimental procedures

2.1. Manufacture of electrodes

A solvent-free electrode rolling technique developed at VARTA [13,14] was adapted by our group to manufacture PEMFC electrodes as described in a previous publication [15]. The catalysts, 20 wt.% Pt and 20 wt.% Pt–Ru supported on Vulcan XC-72 respectively, were mechanically pressed onto a plain weave carbon cloth. (The carbon cloth and catalysts were purchased from E-TEK.) In the case of the Pt–Ru/C electrodes, these two metals were present in a uniform alloy phase according to the manufacturer's X-ray diffraction analysis. The metal loading of the rolled Pt/C electrode was 0.36 mg/cm^2 and that of the Pt–Ru/C electrode was 0.40 mg/cm^2. A commercially available, 20% Pt/C GDE (E-TEK) with 0.4 mg/cm^2 metal loading was tested as well. All electrodes were mounted as a RDE according to the procedure described in Section 2.3.2.

2.2. XPS analysis of Pt / C gas diffusion electrodes

The two electrodes consisting of Pt/C (E-TEK and rolled in-house) were subject to XPS testing. The rolled Pt–Ru/C electrode was not investigated. Samples measuring 1 cm^2 were stamped out from the electrode material. Two E-TEK Pt/C specimens were examined; one as

received, the other was subject to 800 potentiodynamic cycles from 0 to 1.5 V RHE at 100 mV/s in 0.5 M H_2SO_4 with continuous bubbling of Ar before XPS evaluation. Note that this electrode was allowed to dry at room temperature and ambient pressure before testing. Note that all potentials mentioned in this paper are in relation to the reversible hydrogen electrode potential (RHE). The XPS testing procedure was carried out in a similar way to that described in a previous publication from our group using the same equipment [16].

2.3. Half cell electrochemical procedures

2.3.1. Preparation of half cell

Before any experiments were undertaken, all glassware and parts made of Teflon in our half cell were soaked in a 1:1 volumetric mixture of concentrated H_2SO_4 (98%) and HNO_3 (65%) (Merck, pro Analysis grade) to oxidize any organic contaminants that may have harbored. Then they were boiled in de-ionized water for approximately an hour three times. All gas lines were made of Teflon since gas lines made of other materials have been found to be minutely gas permeable. To ensure sterility, powder free gloves were worn while handling all materials at all times.

2.3.2. Mounting of electrodes for half cell analysis

A 1 cm^2 smooth Pt disk was mounted as a RDE embedded in Teflon in a similar way as described by Bard and Faulkner [17]. All other catalyst supported on graphite electrodes were also mounted as RDEs. Round samples of the supported catalyst electrodes measuring 1 cm^2 in area were stamped out and mounted on a steel carrier with an electrically conducting adhesive (Leit-C, Neubauer Chemikalien) used typically to mount specimens for X-ray analysis. Note that this glue was found to be unstable at temperatures above 60°C and therefore no studies were carried out above room temperature. Teflon tape and sleeves were fitted around our electrode to isolate its geometric surface for measurement.

2.3.3. Electrochemical testing procedure

Approximately 100 ml of 0.5 M H_2SO_4 electrolyte was deaerated with Ar (Messer Griesheim, 5.0) for 30 min while rotating the disk electrode at 2000 rpm. Then the smooth Pt RDE was cycled 50 times stationarily from ≈ 0 V to 1.5 V at 100 mV/s in a 1 bar Ar atmosphere at room temperature to odidize any organic impurities before recording 2 cycles at 20 mv/s under the same conditions. Subsequent purging with H_2 (Messer Griesheim, 5.0) for 30 min ensured saturation of the electrolyte for the following procedure: oxidation currents resulting from the potentiodynamic manipulation of the electrode from ≈ 0 V to 300 mV RHE were recorded at various rates of rotation from 100 to 2500 rpm. Then the electrode was conditioned in preparation for a potentiostatic measurement of the

current by evolving H_2 at -20 mV for 5 min at 2000 rpm with continuous H_2 bubbling. After this time period, a H_2 air cushion replaced the bubbling and the rotation was turned off. After 1 min elapsed allowing the solution to equilibrate, a 20 min long chronoamperometric measurement at 180 mV was recorded.

The oxidation of CO on smooth Pt has already been well documented in the literature [7,18–24]. For that reason we do not describe our treatment of this topic nor do we present our findings here.

The E-TEK (20% wt.% Pt/C), rolled Pt/C and Pt–Ru/C electrodes were treated in a similar way with some differences. The electrodes subject to XPS characterization, i.e., the E-TEK and DLR rolled PT/C electrodes, were cycled 800 and 500 times respectively in Ar saturated 0.5 M H_2SO_4 at 100 mV/s non-continuously over a period of three days. During cycling, Ar was bubbled through the electrolyte to deaerate it. A comparison of the behavior of these electrodes over this time period was made. Before the further chronoamperometric and CO stripping experiments were made, the E-TEK electrode was cycled overnight for a total of approximately 2000 cycles. A fresh rolled Pt/C electrode subject to only 100 cycles was used for the further investigations due to the reproducibility of measurements after this low number of cycles. The rolled Pt–Ru/C electrode which was never exposed to a potential more positive than 900 mV to avoid dissolving Ru from the electrode was cycled 100 times before proceeding to the following measurements.

Chronoamperometry was performed on all the porous electrodes in H_2 saturated electrolyte at 180 mV without the pretreatment that the flat Pt electrode received. No potentiodynamic measurements at various rotation speeds of the RDE were taken due to the lack of adherence of non-smooth, porous electrodes to the mass transport relations described by the Levich equation. An attempt was made to simulate a poisoned fuel cell anode by subjecting the E-TEK Pt/C, DLR rolled Pt/C, and DLR rolled Pt–Ru/C electrodes to the following conditions: pure CO (Messer Griesheim, 4.7) was bubbled in the electrolyte for 3 min at 2000 rpm and potentiostating the electrode at 30 mV for 2 min with ongoing CO bubbling and rotation. After adsorbing CO on the surface of the electrode, the electrolyte was cleansed of excess CO for 10 min with Ar at the same potential in preparation for a CO stripping measurement consisting of two cycles over the potential range 10 mV to 1.5 V. All measurements were performed at room temperature.

Data was collected digitally on a IBM PC-compatible computer using m270 software and a potentiostat/galvanostat (model 273) from EG&G Princeton Applied Research. A piece of Pt wire was used as the counter electrode. The mercury/mercurous sulfate reference electrode was separated from the cell by an electrolyte bridge with a porous glass stopper to prevent contamination of the electrolyte via Hg^{2+} ions.

3. Results and discussion

3.1. Smooth PT

We included smooth Pt in our studies to verify the validity of our half cell test set up since experiments on smooth Pt electrodes are already well documented in the literature [17,24–28] before proceeding with our studies on graphite supported electrodes.

3.1.1. Smooth PT in Ar-saturated H_2SO_4

Just as Borup and Vanderborgh [29] found that their membrane electrode assemblies required a 'burn in' period consisting of several hours of operation before repeatable, stable performance was achieved in a single cell, all electrodes we tested in a half cell including smooth platinum required such conditioning to obtain repeatable results. We hypothesize that this electrode conditioning serves to oxidize any organic contaminants in the system and for the supported electrodes, cycling may loan itself to wetting the electrodes, and/or to clearing any PTFE off the surface of Pt or Pt–Ru sites (see Section 3.2). A smooth Pt electrode typically needed at least 50 cycles to obtain consistent results. In the case of Fig. 1, 65 cycles were run before recording this voltamogram.

The roughness factor, R, correlates the geometric and real surface areas. It was calculated according to Eq. (1):

$$R = \frac{Q_H}{Q_{Href} \cdot A} \tag{1}$$

where Q_H corresponds to the amount of charges exchanged during the adsorption of hydrogen atoms on the electrode, $Q_{H\,ref}$ is assumed to be 0.210 mC/cm^2, and A is the electrode's geometric surface area [20]. The value for $Q_{H\,ref}$ assumes that the Pt is polycrystalline having a Pt atom surface density of 1.3×10^{15} atoms per cm^2 [25]. Our sample of polycrystalline Pt had $R = 1.79$.
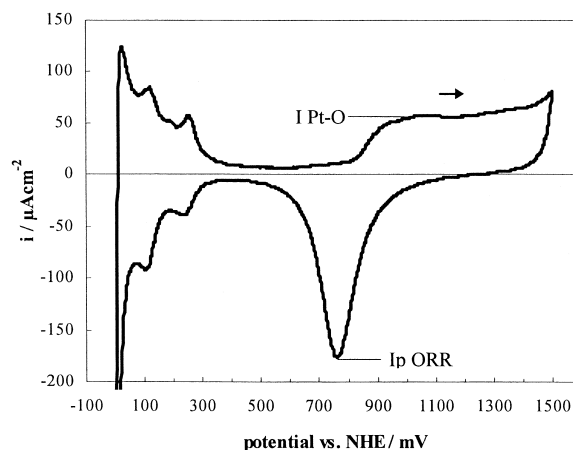

Fig. 1. Cyclic voltammetric current–potential curve for a smooth Pt electrode 0.5 M H_2SO_4 saturated with Ar at 20 mV/s and at room temperature.

3.1.2. Potentiodynamic hydrogen oxidation on smooth Pt in H_2 saturated 0.5 M H_2SO_4

By initially examining the oxidation of hydrogen on smooth, polycrystalline Pt, we were able to verify our ability to perform valid measurements with our setup and to ascertain the cleanliness of our cell, i.e., the purity of the electrolyte and absence of impurities from the system [3]. Furthermore we established that the effect of rotating the electrode and thereby creating a dynamically homogenous electrolytic environment adheres to the predictions of Eq. (2), the Levich equation, which relates the diffusion limited current density, i_l, as a function of the rotation rate, ω (rad s^{-1}) [26]:

$$i_l = 0.620nFD^{2/3}\omega^{1/2}\upsilon^{-1/6}c_o \qquad (2)$$

where n represents the number of electrons in the H_2 oxidation reaction ($n = 2$), F is Faraday's constant ($F = 96484.6$ C/equiv), D is the diffusivity of hydrogen in 0.5 M H_2SO_4 ($D = 3.7 \times 10^{-5}$ cm^2/s) υ is the kinematic viscosity of the electrolyte, 0.5 M H_2SO_4, ($\upsilon = 1.07 \times 10^{-3}$), and c_o is the solubility of H_2 in ($c_o = 7.14 \times 10^{-3}$ M) [3].

The potentiodynamic (20 mv/s) oxidation of hydrogen on a polycrystalline smooth Pt RDE is shown in Fig. 2a. We created a Levich plot (Fig. 2b) from our measurements according to Eq. (3):

$$\frac{1}{i} = \frac{1}{i_k} + \frac{1}{i_l} \qquad (3)$$

where i is the total current density and i_k is the kinetic current density (without the effects of mass transfer) [26]. This equation describes a straight line. The data points for i_l that we obtained via experiment read at 180 mV do generate a line with regression $r^2 = 0.999$ and a slope of 7.10×10^{-2} (mA/cm^2)·rpm$^{-1/2}$. This value is in good agreement ($+8\%$) with the reported theoretical value [3].

Our experiences have shown that a smooth Pt electrode tested without previously being cycled from 0 to 1.5 V in Ar saturated electrolyte do not exhibit such fastidious adherence to the Levich equation. This phenomenon could be due to impurities in the system which are removed only by oxidizing them via cycling.

3.2. Investigation of increasing active surface area on a 20 wt.% Pt / C (E-TEK) electrode

3.2.1. Potendiodynamic cycling of Pt / C electrodes

In performing cyclic voltammetry on the E-TEK electrode, we noticed an increase in the quantity of transferred charge between an as received electrode and one evaluated after running 800 cycles nonconsecutively between ≈ 0 V and 1.5 V at 100 mV/s in 0.5 M H_2SO_4 at room temperature and with ongoing Ar bubbling. Fig. 3a shows the measured currents at the oxide layer reduction peak and at 1180 mV (in the platinum oxide formation area)
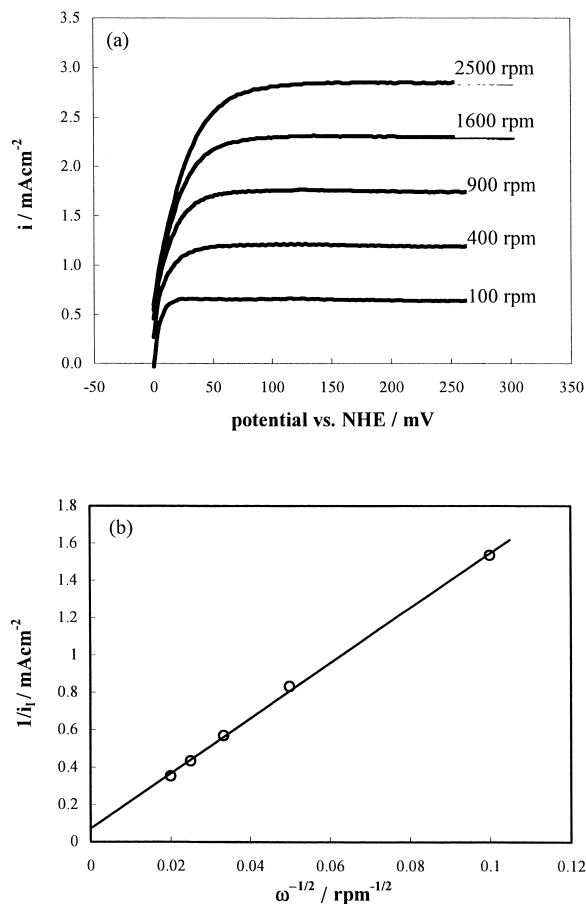

Fig. 2. (a) Hydrogen oxidation currents at various rotation rates on smooth, polycrystalline Pt in H_2 saturated 0.5 M H_2SO_4 at room temperature. (b) A Levich plot at 0.18 V with regression line.

plotted against the number of cycles. The value of both currents became larger throughout the cycling process in a near linear fashion, which indicates that the transferred charge steadily increased and correspondingly the active catalytic surface area got larger. Since the active area increased only while cycling despite the fact that cycling was carried out sporadically over a three day time period, we rule out electrode wetting as a reason for this phenomenon. Potential cycling increases the active area and not the mere soaking of the electrode in the electrolyte.

Fig. 3b shows the results of our DLR rolled Pt/C electrode subject to a similar test as the E-TEK electrode in Fig. 3a. Our electrode's active surface area did not increase much past the first 100 cycles, as exhibited by the values for current in the Pt–O formation (1180 mV) area and at the oxide reduction peak which stayed relatively constant over a three day period. The overall transferred charge and thus surface area also remained steady. Our electrodes which need virtually no conditioning compared to E-TEK's hold much promise in setting new standards for performance. The currents of the DLR Pt/C electrode are an order of magnitude larger than those of the E-TEK electrode, indicating that the active catalytic area is larger.
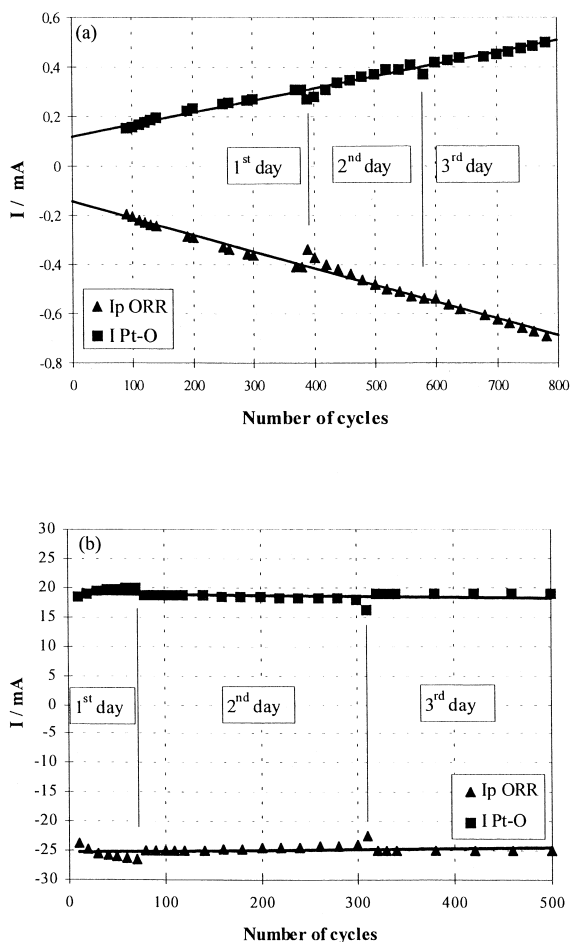
Fig. 3. Current at the oxide layer reduction peak and at 1180 mV (in the platinum oxide formation area) vs. number of cycles for Pt/C electrodes subject to cyclic voltammetry noncontinuously over a 3 day time period between ≈ 0 V and 1.5 V at 100 mV/s in 0.5 M H_2SO_4 with ongoing Ar bubbling and at room temperature. (a) E-TEK 20 wt.% Pt/C electrode. (b) DLR rolled Pt/C electrode.

Upon testing in a fuel cell, the power obtained with our rolled Pt/C electrode is found to be superior to that of the E-TEK electrode at low current densities, as will be presented in a future publication.

Current at the oxide layer reduction peak and at 1180 mV (in the platinum oxide formation area) vs. number of cycles for Pt/C electrodes subject to cyclic voltammetry noncontinuously over a three day time period between ≈ 0 V and 1.5 V at 100 mV/s in 0.5 M H_2SO_4 with ongoing Ar bubbling and at room temperature. (a) E-TEK 20 wt.% Pt/C electrode. (b) DLR rolled Pt/C electrode.

3.2.2. XPS measurements on 20 wt.% Pt/C (E-TEK) electrodes

In the intensity vs. binding energy profiles (Fig. 4) of the E-TEK electrodes obtained from XPS analysis, the F1s signal represents the Teflon which covers the Pt crystallites, which are in turn symbolized by the Pt4f signal. Comparing the relative intensities of the Pt4f and F1s

signals normalized to the F1s peak for both diagrams in Fig. 4 yields an intensity ratio, Pt:F, which is 0.028 in Fig. 4a and 0.129 in Fig. 4b. (Note that the Pt4f signal is amplified ten times in Fig. 4a and five times in Fig. 4b.) The increase of this ratio indicates an enlargement of the exposed surface area of Pt after conditioning due to the disappearance of Teflon. To explain the increase in active catalytic area, it was proposed that organic compounds in the as received E-TEK electrode or from our mounting glue blocked the Pt sites and had to be oxidized away via cycling [30]. It is true that the voltamograms which we recorded that exhibited a continually increasing active surface area with increased cycling could verify this hypothesis, but most organic compounds that could block Pt sites would be vaporized in the ultra-high vacuum chamber of the XPS device. Even if some organic compounds could have survived the ultra-high vacuum chamber then this conjecture could not be correct; if this were the case then as Pt sites cleared up, the ratio Pt:F would increase as the F1s signal remained constant. In practice, the F1s-signal
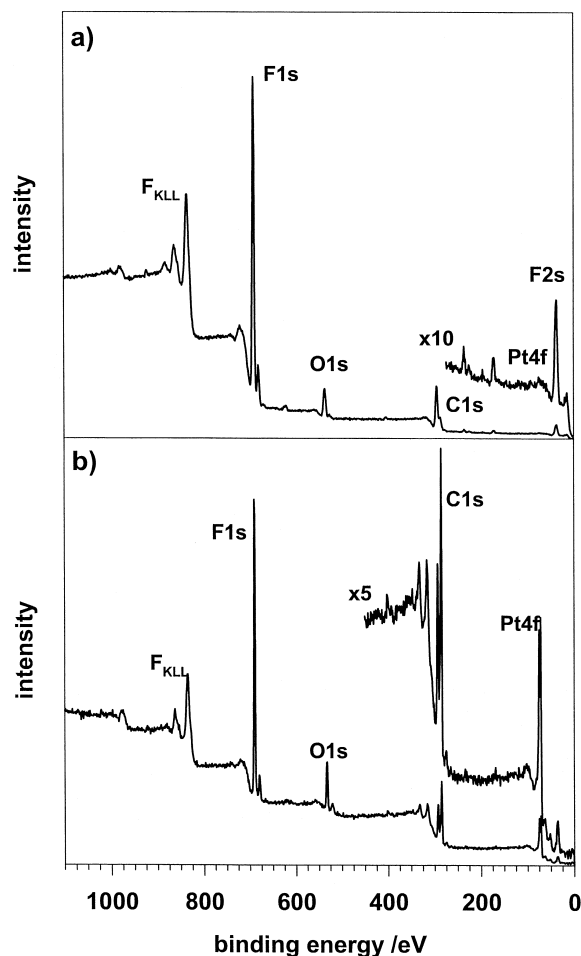

Fig. 4. XPS measurement of Intensity vs. Binding energy of E-TEK electrodes (a) as received and (b) after 800 cycles from ≈ 0 V to 1.5 V at 100 mV/s in 0.5 M H_2SO_4 with ongoing Ar bubbling.
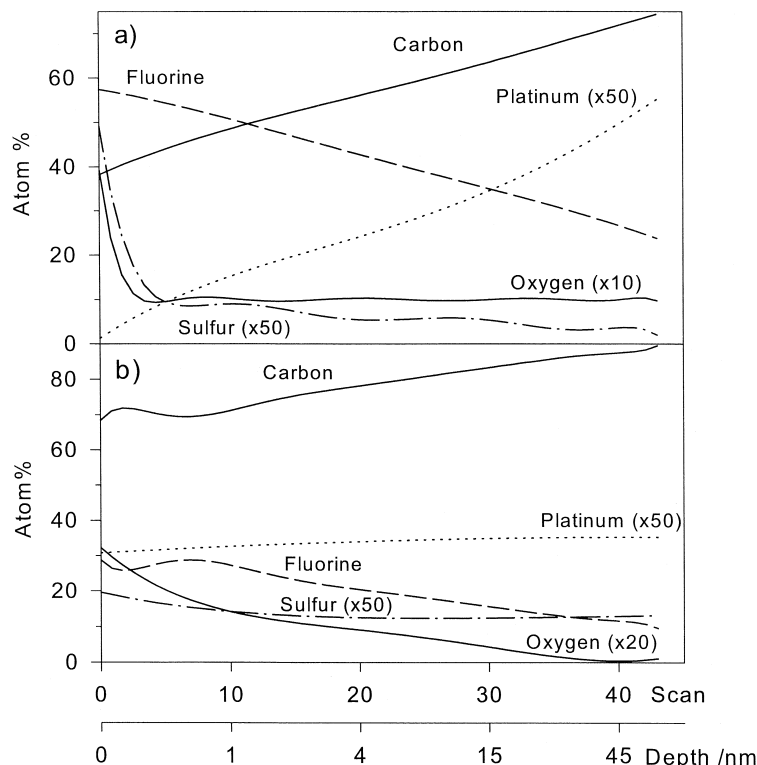
Fig. 5. XPS depth profile of (a) an as received E-TEK Pt/C electrode and (b) a DLR rolled Pt/C electrode.

decreased, verifying our conclusion that the oxidation of organic contaminants was not responsible for the increase in active electrode catalyst surface area but rather the actual Teflon covering of these Pt sites lessened.

Furthermore, in previous XPS studies of E-TEK electrodes, our group has reported the presence of a 3 nm PTFE film covering the surface of the as received electrode [31]. This film covers the active platinum sites as indicated by the depth profile of Pt in the as received E-TEK electrode (Fig. 5a). It shows that the quantity of active Pt sites increases with depth of an as received electrode and that the fluorine content decreases with depth, indicating the diminished presence of PTFE with depth. The depth profile of the cycled E-TEK electrode (not shown), on the other hand, exhibits constant Pt content with increasing depth, as did that of the DLR rolled Pt/C electrode (Fig. 5b). We propose that electrochemical cycling has a similar effect on the PTFE layer covering the surface of the E-TEK electrode to that of the PTFE bonded gas diffusion electrodes for alkaline fuel cells during the reactivation process: the generation of hydrogen gas was found to simultaneously change their pore system and enlarge their active surface area, freeing active sites from PTFE coverage, as mentioned in one our group's previous papers [32]. Since hydrogen was evolved in the E-TEK electrode that was cycled, the mechanism which clears the Pt sites from PTFE could be the similar. The nature of the mechanism causing this phenomenon is unclear, yet we can safely conclude that hydrogen evolution contributes to

the tearing and recession of the PTFE layer around the Pt sites.

3.3. Chronoamperometry in H_2 saturated H_2SO_4

Chronoamperometry measurements were performed to verify the cleanliness of our half cell before proceeding with our CO stripping experiments. Fig. 6 shows that the recorded curves stay relatively constant over time which attests to the cleanliness of the system, i.e., to the lack of impurities which could negatively affect our measurements. Some drop-off of activity during the course of the
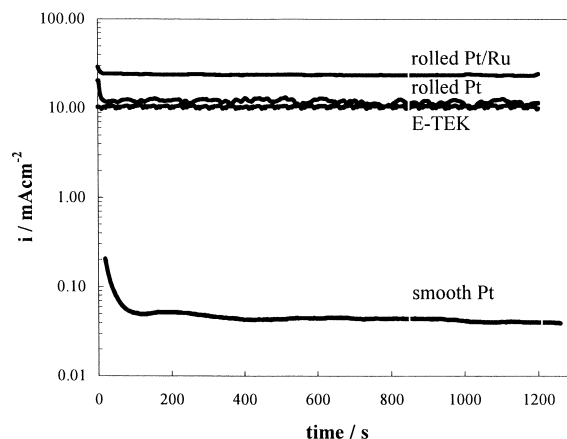

Fig. 6. Chronoamperometry of all tested electrodes at 180 mV in H_2 saturated H_2SO_4 at room temperature without rotation.

measurement is to be expected due to the diminishing concentration gradient of hydrogen in the electrolyte near the electrodes since mass transport was primarily diffusion controlled. The high current densities of the carbon cloth based electrodes are two degrees of magnitude larger than that of smooth Pt. This phenomenon could be due to the fact that H_2 was stored in the pore system of the cloth electrodes [30] and/or merely because the porous electrodes have higher active surface areas for electrocatalysis to occur [33].

3.4. CO stripping voltammetry in 0.5 M H_2SO_4 on porous, supported electrodes

Fig. 7a–c presents the results of our attempts to create and oxidize a monolayer of CO on porous electrodes. The lighter shaded lines in each diagram were the base cyclo-voltamograms recorded in deaerated electrolyte at the sweep rate as with CO. In each case, it is evident that the platinum sites are blocked by CO at the beginning of the first sweep since no hydrogen oxidation is to be seen in the low potential region. Our results are indicative of our difficulties stripping CO from porous electrodes mounted as RDEs. Successful CO stripping depends on the ability to adsorb a monolayer of CO on the catalytic sites of one's working electrode which is oxidized in the first anodic cycle. Obtaining nothing more than a single monolayer on the active sites in the complex pore system of a supported graphite electrode was a difficult challenge. One can see especially in Fig. 7a and c that some residual CO was oxidized in the second sweep, indicating to us that more than a monolayer of CO was present. The highly porous nature of this electrode could result in the absorption and storage of CO in its pore system.

All curves in Fig. 7 exhibit a lack of definition in the CO oxidation peaks and in the hydrogen adsorption and oxidation regions. As a result, we could calculate neither the active surface area, roughness factor, nor the degree of CO-coverage using potentiodynamic techniques. Several reasons could account for the low peak resolution of our samples. Striebel et al. [34] reported that supported electrodes have generally lower peak resolution than smooth electrodes. This finding results from interference on the carbon support of the double-layer charging currents and the less uniform current distribution in a porous electrode than a homogenously exposed smooth electrode. This group also reported that insufficient wetting of the catalyst are could correspond to a lack of peak definition. In addition, Aricò et al. [35] found that a porous electrode's catalytic material is not equally accessible and explained that the electrochemical processes happen at different rates at different depths dependent on the various diffusional stages preceding the reaction at the catalytic sites. Perez et al. also experimentally examined mass transport phenomena within a thin porous coating rotating disk electrode [36]. They created a 'thin film/flooded agglomerate' mathemat-
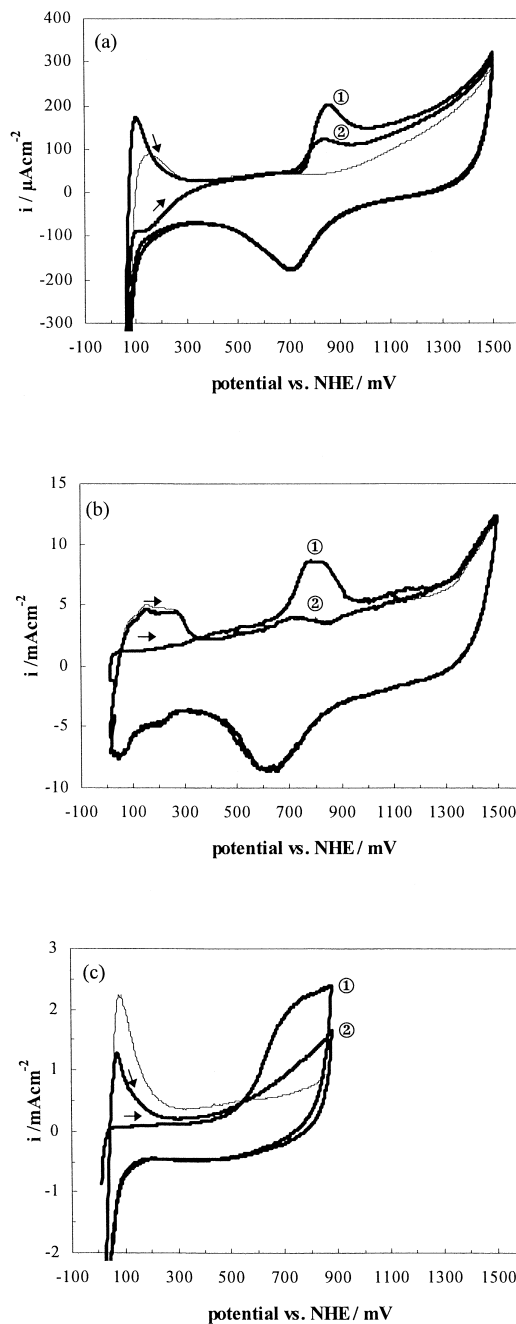

Fig. 7. CO stripping voltammetry of electrodes in 0.5 M H_2SO_4 at 20 mV/s and room temperature (a) E-TEK Pt/C (b) DLR rolled Pt/C (c) DLR rolled Pt–Ru/C.

ical model of the various physical phenomena including diffusional problems occurring within a thin porous coating rotating disk electrode made according to the method described by Tanaka et al. in [37]. All of these reasons contribute to explain the lack of definition in the voltamograms of Fig. 7.

Complications in CO stripping oxidation due to reactant storage in porous electrodes mounted as RDEs could be avoided by using a laboratory set-up like that of Striebel et al. [34]. Doing so would potentially yield results subject to

more extensive interpretation (i.e., with better defined peaks), and eliminate the problems of corrosion and glue dissolution. Perhaps then the CO coverage could be accurately calculated.

The curves in Fig. 7a and b show a peak at 1.5 V, which indicates normal O_2 evolution. Other factors may augment the defined nature of this peak: corrosion of our steel carrier upon which the electrodes were mounted, oxidation of foreign organic matter including < 2 ppm hydrocarbons in our 99.997% pure CO from Messer Griesheim, and the oxidation of our C-substrate [33]. These conjectures represent the speculation of our group; others find nothing unusual about this peak [30].

The most important aspect for the comparison of Pt/C and Pt–Ru/C electrodes is the difference in the peak potential. Fig. 7a shows the Pt supported on graphite E-TEK electrode, whose CO oxidation peak lies at approximately 850 mV, a value 100 mV above the results reported for pure smooth Pt [3]. This graph indicates that residual CO was oxidized during the second sweep. As previously mentioned, the pore system harbored excess CO, in which case an anodic shift of the peak is to be expected as evidenced in prior studies on smooth electrodes in CO saturated electrolyte [3]. That of the DLR rolled Pt/C electrode in Fig. 7b, located at approximately 780 mV, agrees well with the reported result. The activity seen above 1.0 V is characteristic of organic compounds; we suspect our mounting glue to be the culprit [33]. The DLR rolled Pt-Ru/C electrode in Fig. 7c had a CO oxidation peak starting at 560 mV but did not show a definite peak, perhaps due to organic species present in the system [33]. The Ru present reduces the overpotential for CO oxidation, but a comparison with the reported starting point of CO oxidation on smooth 50% Ru indicates that our porous electrode does not do so as effectively; it starts CO oxidation 150 mV later at a more anodic potential [3].

4. Conclusions

Cyclic voltammetry is an extremely useful technique on account of its high sensitivity. To employ this method for characterization of electrodes in face of CO poisoning, utmost care must be taken that the electrolyte, electrodes, experimental equipment, and CO gas are free from organic impurities which influence CV measurements. Voltamograms are dependent among other things on catalyst loading, electrode structure and the manner in which the sample electrode has been handled prior to recording the voltamogram [15]. The manner in which electrodes were catalyzed (i.e., batch ink process vs. continuous rolling process) also influence potentiodynamic measurements.

XPS and cyclic voltammetry measurements have indicated the Pt surface area on an E-TEK Pt electrode increases via electrochemical cycling because the PTFE covering the surface seems to diminish. Hydrogen evolu-

tion contributes to the degradation of this layer as was found to be the case with alkaline fuel cell electrodes during reactivation [32].

The results from the half cell in a liquid sulfuric acid medium cannot be fully projected to single cell measurements with a solid polymer electrolyte since in the half cell, H_2 is dissolved in H_2SO_4 whereas in a complete cell H_2 is mostly gaseous. In addition, at low current densities where the reaction kinetics are limiting, comparisons between the half and full cells might be possible; at higher current densities typical found in complete cells, however, complicated mass transport operations contribute to overpotentials. Electrodes in a half cell exhibit totally different mass transport conditions. For prescreening purposes, half cell studies are quicker than full cell studies, but the results allow only permit a limited degree of qualitative projection to a full cell.

Potential further areas of study include re-testing the same porous electrodes mounted as GDEs. In addition, XPS could be performed on the DLR rolled Pt–Ru/C electrode before and after cycling in a half cell to examine the physical changes on the electrode surface that potentiodynamic measurements may cause.

References

[1] International Energy Agency, World Energy Outlook 1994 edn., OECD/IEA, 1994, pp. 18.
[2] D.W. McKee, A.J. Scarpellino Jr., Electrochem. Tech. 6 (1998) 101–105.
[3] H. Gasteiger, N. Markovic, P.N. Ross, J. Phys. Chem. 99 (1995) 8290–8301.
[4] H. Gasteiger, N. Markovic, P.N. Ross, E. Cairns, J. Phys. Chem. 98 (1994) 617–625.
[5] H. Gasteiger, N. Markovic, P.N. Ross, J. Phys. Chem. 99 (1995) 8945–8949.
[6] K. Wang, H. Gasteiger, N. Markovic, P.N. Ross, Electrochim. Acta 41 (16) (1996) 2587–2593.

[7] M.J. Weaver, S.C. Chang, L.W. Leung, X. Jiang, M. Rubel, M. Szklarcyk, D. Zurawski, A. Wieckowski, J. Electroanal. Chem. 327 (1992) 247–260.

[8] H. Gasteiger, N. Markovic, P.N. Ross, Tagungsband der 4. Ulmer ElectroChemischen Tagen, 1996, pp. 193–206.

[9] D.P. Wilkinson, D. Thompsett, in: O. Savadogo, P.R. Roberge (Eds.), Proceedings of the Second International Symposium on New Materials for Fuel Cell and Modern Battery Systems, Ecole Polytechnique de Montreal, 1997, pp. 266–285.

[10] H.F. Oetjen, V.M. Schmidt, U. Stimming, F. Trila, J. Electrochem. Soc. 143 (1996) 3838–3842.

[11] T.R. Ralph, Plat. Met. Rev. 41 (3) (1997) 102–113.

[12] G. Tamizhmani, J.P. Dodelet, D. Guay, J. Electrochem. Soc. 143 (1) (1996) 18.

[13] H. Sauer, (Varta), Apparatus and method for a plastic-bound activated carbon layer for thin gas diffusion electrodes, Ger Offen. 2 941 774 (Cl. H01M4/88), Apr. 30, 1981, Appl. Oct 16, 1979, 9 pp.

[14] A. Winsel (Varta), Porous Gas Electrodes, Ger Offen. DE 3 342 969 (Cl. C25B11/06), Jun. 5, 1985, Appl. Nov. 28, 1983, 12 pp.

[15] D. Bevers, N. Wagner, M. von Bradke, J. Hydrogen Power 63 (1996) 193–201.

[16] M. Schulze, K. Bolwin, E. Gülzow, W. Schnurnberger, Fresnius J. Anal. Chem. 335 (1995) 778–784.

[17] A. Bard, L. Faulkner, Electrochemical Methods, Fundamentals and Applications, Wiley, 1980, p. 283.

[18] O. Wolter, J. Heitbaum, Ber. Bunsenges. Phys. Chem. 88 (1984) 6–10.

[19] M. Hachkar, T. Napporn, J.-M. Léger, B. Beden, C. Lany, Electrochim. Acta 41–17 (1996) 2721–2730.

[20] J.Y. Tilquin, R. Côté, D. Guay, J.P. Dodolet, G. Denès, J. Power Sources 61 (1996) 193–200.

[21] H.P. Dhar, L.G. Christner, A.K. Kush, H.C. Maru, J. Electrochem. Soc. (1986) 1574–1582.

[22] S.A. Bilmes, N.R. de Tacconi, A.J. Arvía, J. Electrochem. Soc. 127 (10) (1980) 2184–2187.

[23] H. Igarashi, T. Fujino, M. Watanabe, J. Electroanal. Chem. 391 (1995) 119–123.

[24] J.M. Feliu, J.M. Orts, A. Fernandez-Vega, A. Aldaz, J. Electroanal. Chem. 296 (1990) 191–201.

[25] R. Woods, Electroanal. Chem. 9 (1976) 57.

[26] Bard and Faulkner, p. 288.

[27] C. Hamann, W. Vielstich, Elektrochemie II, Elektroden Prozesse, Angewandte Elektrochemie, Verlag Chemie, 1981, pp. 51–52.

[28] H. Angerstein-Kozlowska, B.E. Conway, W.B.A. Sharp, Electroanal. Chem. and Interfac. Electrochem. 43 (1973) 9–36.

[29] R.L. Borup, N.E. Vanderborgh, Electrochem. Soc. Proc. 95–23 (1995) 168.

[30] H. Gasteiger, private communication, Germany, 1997.

[31] M. Schulze, N. Wagner, G. Steinhilber, E. Gülzow, M. Wöhr, K. Bolwin, Proc. Fuel Cell Seminar, Orlando, 1996, pp. 663–667.

[32] E. Gülzow, B. Holzwarth, W. Schnurnberger, M. Schulze, G. Steinhilber, N. Wagner, Hydrogen Energy Progress IX, Proc. World Hydrogen Energy Conference, Vol. 3, Paris, 1992, pp. 1507–1515.

[33] S. Srinivasan, private communication, France, 1997.

[34] K. Striebel, F. McLarnon, E. Cairns, J. Electrochem. Soc. 137 (11) (1990) 3360–3367.

[35] A. Aricò, V. Alderucci, V. Antonucci, S. Ferrara, V. Recupero, N. Giordano, K. Kinoshita, Electrochimica Acta. 37 (3) (1992) 527.

[36] J. Perez, A. Tanaka, E. Gonzalez, e. Ticianelli, J. Electrochem. Soc. 141 (2) (1994) 431–436.

[37] A. Tanaka, C. Fierro, D. Scherson, E. Yeager, J. Phys. Chem. 91 (1987) 3799–3807.